A structural study of the aqua-anions NO_3^-, BrO_3^- and ClO_3^- by difference methods of X-ray diffraction

1991 J. Phys.: Condens. Matter 3 837

(http://iopscience.iop.org/0953-8984/3/7/008)

J. Phys.: Condens. Matter 3 (1991) 837–850. Printed in the UK

A structural study of the aqua-anions NO_3^-, BrO_3^- and ClO_3^- by difference methods of x-ray diffraction

C A E Burke, A K Adya† and G W Neilson

H H Wills Physics Laboratory, University of Bristol, Tyndall Avenue, Bristol BS8 1TL, UK

Received 5 September 1990, in final form 5 December 1990

Abstract. The method of x-ray diffraction with isomorphic substitution has been extended to aqueous solutions containing complex ions. In a study of isomorphism between NO_3^-(aq), BrO_3^-(aq) and ClO_3^-(aq), it is found that the NO_3^- and BrO_3^- ions are isomorphic up to the level of the first-order difference indicating a similarity in their anion-hydration structure. Based on the isomorphism of these two ions, and because the water molecules are only weakly perturbed from their structure in pure water, a second-order difference calculation was made and the ion–ion pair correlation function of these two ions obtained. The results show that the most probable ion–ion separation is between 5 Å and 11 Å and the distance of closest approach is 4.8 Å. NO_3^- and BrO_3^- are found, however, not to be isomorphic with ClO_3^-.

1. Introduction

The x-ray first- and second-order difference techniques of isomorphic substitution (Skipper 1987) have been successfully tested and applied previously to various cationic species in aqueous solution such as Ni^{2+}(aq) and Mg^{2+}(aq) ($Ni/MgCl_2$, $Ni/MgBr_2$: Skipper 1987, Skipper *et al* 1986, 1989), Ni^{2+}(aq) and Mg^{2+}(aq) ($Ni/MgSO_4$ and $Ni/Mg(NO_3)_2$: Burke 1989), Na^+(aq) and Ag^+(aq) ($Na/AgNO_3$: Skipper 1987 and Skipper and Neilson 1989), Rb^+(aq) and Tl^+(aq) (RbOH and TlOH: Adya and Neilson 1991) and were used to derive ion–ion correlation functions. Here, we extend these techniques to investigate the existence of isomorphism between the complex anionic species NO_3^-(aq), BrO_3^-(aq) and ClO_3^-(aq) and then to exploit the isomorphism obtained to derive the anion–anion pair correlation function.

In the crystalline state $NaNO_3$, $NaBrO_3$ and $NaClO_3$ are known to be isomorphous (Wyckoff, 1964), each having a NaCl-like structure. Various properties of the NO_3^-(aq), BrO_3^-(aq) and ClO_3^-(aq) ions are given in table 1. For equivalent structural studies in aqueous solution, the choice of NO_3^- and BrO_3^- as a possible isomorphic pair was based on these anions having the same valence and similar effective ionic radii, r_{eff} (Yatsimirskii 1947, 1948, Huheey 1978, Waddington 1959), 1.89 and 1.91 Å respectively. It should be noted, however, that in the crystalline state the intramolecular central atom–O, X–O, distances are not similar, as expected, and are $r_{NO} = 1.217$ Å

† Permanent address: Kirori Mal College, University Enclave, University of Delhi, Delhi-110007, India. Present address: School of Chemistry, University of Bristol, Cantock's Close, Bristol BS8 1TS, UK.

0953-8984/91/070837+14$03.50

Table 1. Various properties of the NO_3^-, BrO_3^- and ClO_3^- ions. r_{XO} is the crystalline X–O distance and r_{eff} is the effective ionic radius, Huheey (1978), Waddington (1959) and Yatsimirskii (1947, 1948).

Ion	r_{XO} (Å)	Shape	O–X–O (deg)	r_{eff} (Å)
NO_3^-	1.217[a]	Planar equilateral triangle	120	1.89
BrO_3^-	1.663[b]	pyramidal	104.6	1.91
ClO_3^-	1.49[c]	pyramidal	106.8	2.00

[a]Wyckoff (1964).
[b]Templeton and Templeton (1985).
[c]Burke-Laing and Trueblood (1977).

and $r_{BrO} = 1.663$ Å respectively, table 1. Their structures are also different, the NO_3^- ion being a planar equilateral triangle, and the BrO_3^-, pyramidal.

The ClO_3^- ion was chosen as a possible isomorph with the NO_3^- ion because within the context of NO_3^- uptake in plants, Deane-Drummond and Glass (1982) found that ClO_3^- acts as an analogue for NO_3^-, i.e., plants cannot distinguish between the two ions and concluded that the hydrated molecular dimensions of these ions are very similar. A similar study of the BrO_3^- ion shows that it is not an analogue for the NO_3^- ion. Despite this observation, however, the possibility of isomorphism between ClO_3^- and NO_3^- must be considered in light of the observations that the ClO_3^- has a flat trigonal pyramid structure with an intramolecular separation of 1.49 Å. It must be noted here, though, that its effective ionic radius is different, $r_{eff} = 2.0$ Å (Huheey 1978).

For completeness, the hydration structures of BrO_3^- and ClO_3^- were tested for possible isomorphic behaviour. They both have a pyramidal structure, and their intramolecular ion–O distances in the crystalline state are closer (1.663 Å and 1.49 Å) than for the other combination of pairs.

2. Theoretical background

2.1. Diffraction from an aqueous solution with a complex anion

For an aqueous electrolyte solution with a complex anion, MXO_n in H_2O, there are ten differently weighted partial structure factors, $g_{ab}(r)$, contributing to the total structure factor. These functions can be related to the x-ray or neutron structure factors of the sample, $F^x(k)$ or, $F^n(k)$, where superscripts x and n denote x-ray and neutron data respectively. This is obtained from the experimental intensity, $I(k)$

$$F(k) = \alpha(k)[I(k) + \gamma(k)] \tag{1}$$

where $k = 4\pi \sin\theta/\lambda$ and is the scattering wavenumber, $\hbar k$ is the momentum transfer of x-rays or neutrons of wavelength λ, scattered through an angle 2θ, and $\alpha(k)$ and $\gamma(k)$ represent correction functions which must be used to obtain a properly normalised structure factor (Enderby and Neilson 1981). $F(k)$ is defined as

$$F(k) = \sum_{a=1}^{m}\sum_{b=1}^{m} c_a c_b f_a(k) f_b(k)[S_{ab}(k) - 1] \tag{2}$$

where $f_a(k)$ is a form factor of species a if x-ray scattering is being considered or the scattering length of a nucleus of species a if neutron scattering is being considered, c_a is the atomic fraction of scattering centres of species a and the summations are over the total number of species m. $S_{ab}(k)$ is the partial structure factor of species a and b, related to $g_{ab}(r)$ by the Fourier transformation

$$g_{ab}(r) - 1 = \frac{1}{2\pi^2 \rho r} \int_0^\infty [S_{ab}(k) - 1] \sin(kr) k \, \mathrm{d}k \tag{3}$$

where ρ is the total number density of particles in the system and is ≈ 0.1 Å^{-3} for an aqueous solution.

2.2. The difference method for a solution containing a complex anion

At the first-order difference level, the difference between the two $F^x(k)$ gives information about the ion–solvent structure yielding $\tilde{\Delta}^x(k)$. The first-order differences used are

$$\tilde{\Delta}^x(k)_1 = F_I^x(k) - F_{II}^x(k) \tag{4}$$
$$\tilde{\Delta}^x(k)_2 = F_I^x(k) - F_{III}^x(k) \tag{5}$$
$$\tilde{\Delta}^x(k)_3 = F_{III}^x(k) - F_{II}^x(k) \tag{6}$$

where I is the solution containing the ion which is the stronger scatterer, X, II is the solution with the weaker scatterer, X′, and III contains the 50:50 mixture. The first-order differences are defined as

$$\tilde{\Delta}^x(k) = A(k)[\tilde{S}_{XO}(k) - 1] + B(k)[\tilde{S}_{XH}(k) - 1] + C(k)[\tilde{S}_{XM}(k) - 1] + D(k)[\tilde{S}_{XX}(k) - 1]. \tag{7}$$

The coefficients of equation (7) are defined as

$$A(k) = 2c_O c_X f_O(k) f_X(k) \Delta f_X(k) \tag{8}$$
$$B(k) = 2c_H c_X f_H(k) f_X(k) \Delta f_X(k) \tag{9}$$
$$C(k) = 2c_M c_X f_M(k) f_X(k) \Delta f_X(k) \tag{10}$$
$$D(k) = c_X^2 (\Delta f_X(k))^2 \tag{11}$$

where

$$\Delta f_X(k) = f_X(k) - f_{X'}(k) \tag{12}$$
$$(\Delta f_X(k))^2 = (f_X(k))^2 - (f_{X'}(k))^2 \tag{13}$$

Even though the difference is a convoluted distribution function, by dividing through by A(k), a new function, $\tilde{\Delta}_{XO}(k)$, is created. This allows the X–O term to be deconvoluted and therefore investigated

$$\tilde{\Delta}_{XO}^x(k) = [\tilde{S}_{XO}(k) - 1] + \left(\frac{B(k)}{A(k)}\right)[\tilde{S}_{XH}(k) - 1] + \left(\frac{C(k)}{A(k)}\right)[\tilde{S}_{XM}(k) - 1] + \left(\frac{D(k)}{A(k)}\right)[\tilde{S}_{XX}(k) - 1] \tag{14}$$

where

$$\tilde{S}_{X\alpha}(k) = S_{X\alpha}(k) - [S_{X'\alpha}(k) - S_{X\alpha}(k)][f_{X'}(k)/(f_X(k) - f_{X'}(k))] \tag{15}$$

since $S_{X'\alpha}(k) \neq S_{X\alpha}(k)$ if X′ and X are not perfect isomorphs. α = M, H or O and

$$\tilde{S}_{XX}(k) = S_{XX}(k) - [S_{X'X'}(k) - S_{XX}(k)][f_{X'}^2(k)/(f_X^2(k) - f_{X'}^2(k))]\,. \tag{16}$$

The Fourier transform of $\tilde{\Delta}_{XO}(k)$ is

$$\tilde{G}_{XO}(r) = [\tilde{g}_{XO}(r) - 1] + \frac{1}{2\pi^2\rho r}\int_0^\infty \left(\frac{B(k)}{A(k)}[\tilde{S}_{XH}(k) - 1] + \frac{C(k)}{A(k)}[\tilde{S}_{XM}(k) - 1] + \frac{D(k)}{A(k)}[\tilde{S}_{XX}(k) - 1]\right) \tag{17}$$

and

$$\tilde{G}_{XO}(r) = \tilde{g}_{XO}(r) + \frac{A(0) + B(0) + C(0) + D(0)}{A(0)} + \int [H_{B,A}|r - r'|\tilde{g}_{XH}(r') + H_{C,A}|r - r'|\tilde{g}_{XM}(r') + H_{D,A}|r - r'|\tilde{g}_{XX}(r')\,dr'] \tag{18}$$

where

$$\tilde{g}_{ab}(r) = g_{ab}(r) - \int_{-\infty}^{\infty}[g_{a'b}(r) - g_{ab}(r)]H_{f',f-f'}|(r - r')|dr' \tag{19}$$

where a is a stronger scatterer than b, and $f = f_a(k)$ and $f' = f_b(k)$. $H_{Y,Z}\,|r - r'|$ is defined as

$$H_{Z,Y}(r) = \frac{2}{\pi}\int_{-\infty}^{\infty}\frac{Z(k)}{Y(k)}\cos(kr)\,dk\,. \tag{20}$$

Skipper (1987) shows the effects of these functions.

At the second-order difference level, the X–X structure factor, $\tilde{S}_{XX}(k)$, can be determined, and hence also the Fourier transform, $\tilde{g}_{XX}(r)$. $\tilde{S}_{XX}(k)$ is defined as

$$\tilde{S}_{XX}(k) - 1 = \frac{1}{c_X^2}\left(\frac{(F_I(k) - F_{II}(k))}{(f_X - f_{X'})} - \frac{(F_I(k) - F_{III}(k))}{(f_X - f_{X/X'})}\right). \tag{21}$$

In neutron isotopic substitution experiments, $f_X(k)$ and $f_{X'}(k)$ are independent of k. However, for x-ray diffraction, $f_X(k)$ is a k-dependent atomic form factor. Thus Fourier transformation of $F_X(k)$ will involve convolutions of the partial structure factors with the corresponding $f_X(k)$. Recall that $f_X(k)$ is proportional to electron number and thus interchanging one species for another which has different scattering properties, will not necessarily lead to the same structure in solution.

In 1970, Bol *et al* developed a method based on isomorphic substitution to overcome this problem. They were thus able to come to a better understanding of cation hydration than before. However, they did not carry out any independent checks on their results. Skipper (1987) and Skipper *et al* (1989) developed a method based on isomorphic substitution and x-ray diffraction, the results have been compared with the formally exact difference method of neutron diffraction. Checks for self-consistency were also made between the three difference functions (equations (4)–(6)).

3. Experimental method

3.1. The samples

The samples were made in our chemical laboratory at Bristol from salts obtained from BDH Limited. De-ionized water was used in every case. The final solutions were placed in glass flasks or bottles and placed in an ultra-sound bath for at least 5 min to make sure that each salt was completely dissolved and to remove all air bubbles.

3.2. The experimental set-up

X-ray diffraction experiments were carried out on six aqueous solutions: $NaBrO_3$, I; $NaNO_3$, II; a 50:50 mixture of $NaBrO_3$ and $NaNO_3$, III; $NaClO_3$, IV; a 50:50 mixture of $NaNO_3$ and $NaClO_3$, V; a 50:50 mixture of $NaBrO_3$ and $NaClO_3$, VI. The properties of these solutions are given in table 2. All the solutions were 1M in concentration because $NaBrO_3$ is insoluble above 1.822M (*Handbook of Chemistry and Physics* 1988), and 1M is far enough away from this limit but the solution still gives sufficient counting statistics. The method of isomorphic substitution was then applied to the pairs NO_3^- and BrO_3^-, NO_3^- and ClO_3^-, and BrO_3^- and ClO_3^-.

Table 2. Properties of the solutions used in the x-ray experiments. ρ = sample density, μ = linear absorption coefficient, V = average volume of an atom.

Solution	Label	ρ (g cm^{-3})	μ (g cm^{-2})	V (Å^3)
1M $NaBrO_3$	I	1.112	7.109	10.061
1M $NaNO_3$	II	1.052	1.159	10.002
1M $NaNO_3/BrO_3$	III	1.083	4.135	10.021
1M $NaClO_3$	IV	1.070	1.557	10.041
1M $NaNO_3/ClO_3$	V	1.062	1.359	10.009
1M $NaClO_3/BrO_3$	VI	1.088	4.330	10.079

A neutron diffraction experiment was carried out on one of the samples, using the formally exact method of isotopic substitution. In this case a 4.32m $Ni(NO_3)_2$ solution (Howell 1990) was used in which a replacement of ^{14}N by ^{15}N enabled the difference functions $\Delta^n_{XO}(k)$ and hence $g^n_{XO}(r)$ to be obtained (superscript n denotes a result due to neutron diffraction). These results are only used as a comparison with the x-rays, and will be published at a later date as they are interesting in their own right.

X-ray diffraction data were obtained for the six equi-molar aqueous solutions at room temperature (24 ± 4) °C on a $\theta - \theta$D/MAX diffractometer manufactured by the Rigaku Corporation, Japan. All the experiments were carried out in reflection mode using an approximation to the Bragg-Brentano para-focussing method (Cullity 1956). With this geometry the x-rays are diffracted from a horizontal surface in the liquid and the x-ray source and detector arms subtend an angle $\theta°$ to the free surface of the liquid sample. The reflection geometry and slit arrangement is also used since it completely eliminates sample holder absorption and scattering. The system was calibrated with silicon powder.

X-rays of wavelength 0.7107 Å were produced by a Mo target x-ray tube operated at 50 kV and 40 mA. A zirconium filter was placed in the beam to remove Mo K_β radiation. A focussing graphite monochromator was placed in the reflected beam to

reduce Compton scattering and background radiation. The cell used was circular with a diameter of 8 cm and was made of either brass or glass with a window of aluminium (thickness 0.025 mm) sealed onto the cell with vacuum grease.

100 000 counts were collected per angle over the range $2° < 2\theta < 156°$, i.e., $0.3\ Å^{-1} < k < 17.5\ Å^{-1}$, with a step of 0.2°. Several scans were taken for each angle range over a few days rather than one long scan for each range and the sample was checked each time in between these scans. This was done so that the consistency between the different scans could be checked and so as to minimise the effects due to evaporation of the sample at the surface. At this time, no method of temperature control was employed. By cycling the angle range scans, an average over the range of temperatures could be taken.

3.3. Data analysis

The data were corrected for background, multiple scattering, absorption, polarization, Compton scattering and incoherent scattering using the procedures described by Skipper (1987). They were normalized to electrons, $e^2\ Å^{-3}$, by the method of Habenschuss and Spedding (1979), and the total structure factor, $F^x(k)$, of each solution was determined. It should be noted here that atomic scattering factors exist only for an oxygen atom and an oxygen ion (Cromer 1969, *International Tables for X-ray Crystallography* 1962) and a decision was taken to split the anion into a central atom, X, $(n-1)$ neutral oxygen atoms, O′, and one O^- ion giving the complex anion its negative charge. In reality this charge will be shared by the three oxygens. As regards normalization of the data, the procedure used by Skipper (1987) was not followed exactly here; instead the final form factor fit, $X(k)$, through the data, $I^x(k)$, was chosen when the r-space Fourier transform of $I^x(k) - X(k)$ had a minimum amount of noise at values of low r, and a coordination number of 2 hydrogens around the oxygen for the intramolecular O–H peak at ≈ 1 Å. In table 3 the coordination numbers obtained for each solution for the O–H interaction are listed.

Table 3. Water parameters for each solution.

Solution	Label	r_{OH} (Å)	n_{OH}
1M $NaBrO_3$	I	0.97	1.86(1)
1M $NaNO_3$	II	1.03	1.95(1)
1M $NaNO_3/BrO_3$	III	1.03	2.34(1)
1M $NaClO_3$	IV	0.89	1.72(1)
1M $NaNO_3/ClO_3$	V	1.03	2.14(1)
1M $NaClO_3/BrO_3$	VI	0.97	2.31(1)

4. Results and discussion

4.1. Isomorphism of NO_3^-, BrO_3^-, and ClO_3^-

The $F^x(k)$ obtained for each of the six solutions are shown in figure 1. The structure factors for solutions I, II and III, $F^x(k)_I$, $F^x(k)_{II}$ and $F^x(k)_{III}$ respectively show similar peaks and troughs at ≈ 2, 3 and 5 $Å^{-1}$, but there are slight displacements of peak and trough positions in the structure factors of solutions IV, V and II, $F^x(k)_{IV}$,

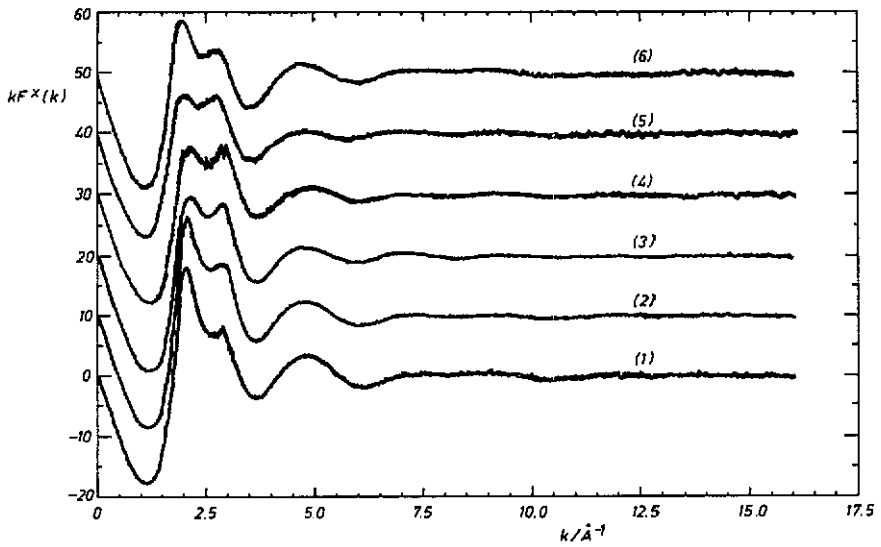

Figure 1. The structure factors, $kF^x(k)$, for 1M $NaNO_3/BrO_3/ClO_3$. Curve 1, $kF^x(k)_I$; curve 2, $kF^x(k)_{III}$ (displaced by + 10 e^2 $Å^{-1}$); curve 3, $kF^x(k)_{II}$ (+ 20 e^2 $Å^{-1}$); curve 4, $kF^X(k)_{IV}$ (+ 30 e^2 $Å^{-1}$); curve 5, $kF^X(k)_V$ (+ 40 e^2 $Å^{-1}$); curve 6, $kF^X(k)_{VI}$ (+ 50 e^2 $Å^{-1}$).

$F^x(k)_V$ and $F^x(k)_{II}$, and similarly of solutions I, IV and VI, i.e., $F^x(k)_I$, $F^x(k)_{IV}$ and $F^x(k)_{VI}$, respectively. The $F^x(k)$ are Fourier transformed and the total pair distribution functions, $G^x(r)$, are obtained, and represent the average structure of the solution. This is far too ambiguous to be determined directly, apart from the intra-molecular O–H water peak at $\approx$ 1 Å. The intra-molecular and inter-molecular X–O correlations cannot be determined at this stage because of the underlying water–water correlations. Sandström *et al* (1985) showed there is no strong Ag^+–O correlation and since Skipper and Neilson (1989) have shown that Na^+ is isomorphic with Ag^+, then it can be concluded that there is no strong Na^+–O correlation. Thus a reliable Na^+–O correlation cannot be determined either.

The three sets of x-ray diffraction first-order difference results, $k\tilde{\Delta}(k)$, are shown in figures 2, 3 and 4. Figure 2 shows the $k\tilde{\Delta}(k)$ for I – II, I – III, and III – II. These show very good agreement with peaks and troughs at 2, 3 and 5 $Å^{-1}$ and so on, indicating no major structural difference between the three solutions. The corresponding Fourier transforms, $\tilde{G}^x_{XO}(r)$, are shown in figure 5 which again show similar structures. In table 4, the parameters of these $\tilde{G}^x_{XO}(r)$ are listed giving the average intramolecular distance of the oxygens to the X atom as 1.63 Å and the coordination number as 3.17(54) and the intermolecular distance of the oxygens of the water molecule as 3.46(1) Å. These results are consistent with those of Neilson and Enderby (1982)(7.8m $NaNO_3$), Walker *et al* (1988) (18m and 12m ND_4NO_3) and Howell (1990)(4.3m $NiNO_3$), where m denotes molality of the solution. Walker *et al* identify the range from 2.14 to 3.0 Å as being due to X–D correlations, where D is a constituent of the ND_4^+ ion. A peak at $\approx$ 2.8 Å is seen in both sets of Walker's data increasing in size with a decrease in concentration, which Walker *et al* also attribute to these X–D correlations. This is also seen in our data at $\approx$ 2.90(8) Å and in the data of Howell at 3.09 Å. However, since the ND_4^+ ion is not present in Howell's and

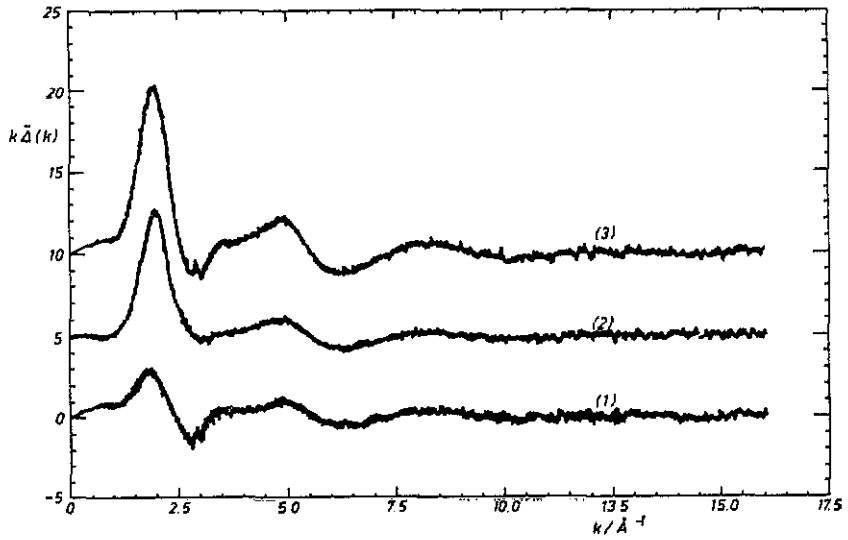

Figure 2. The first-order difference functions, $k\bar{\Delta}(k)$, for 1M $NaNO_3/BrO_3$. Curve 1, results for solution (I – III); curve 2, those for solutions (III – II) (displaced by 10 e^2 $\AA^{-1}$); curve 3, those for solutions (I – II) (displaced by 20 e^2 $\AA^{-1}$).

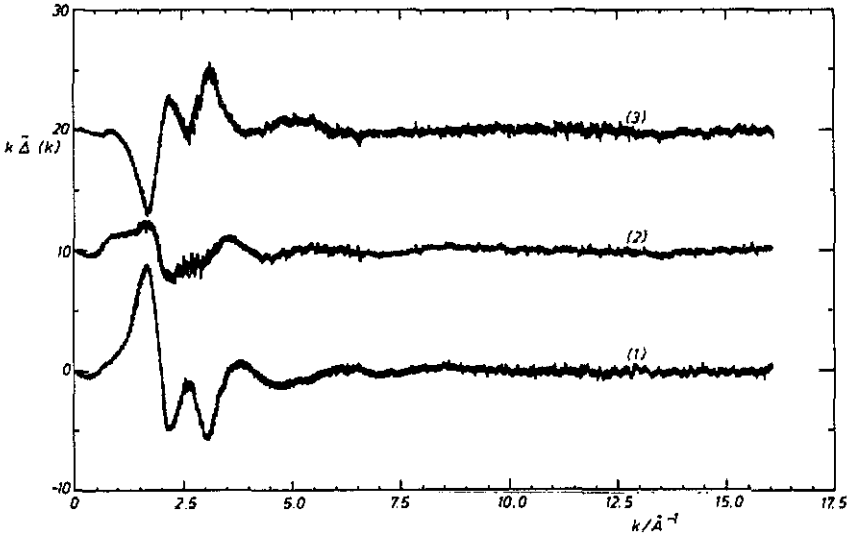

Figure 3. The first-order difference functions, $k\bar{\Delta}(k)$, for 1M $NaNO_3/ClO_3$. Curve 1, results for solution (V – II); curve 2, those for solutions (IV – II) (displaced by 10 e^2 $\AA^{-1}$); curve 3, those for solutions (IV – V) (displaced by 20 e^2 $\AA^{-1}$).

our data, this peak must be due to another interaction. Thus it is probably due to the X–D interaction where the deuterium belongs to the heavy water molecules weakly coordinated to the X atom in the neutron case and hence in our data, the X–H interaction, where the H is from the hydrogen in the water. This would justify the increase in peak size with decreasing concentration. The X–D_2O (X–H_2O) interactions in this region (2 to 5 Å) were originally suggested by Caminiti *et al* (1980) and later

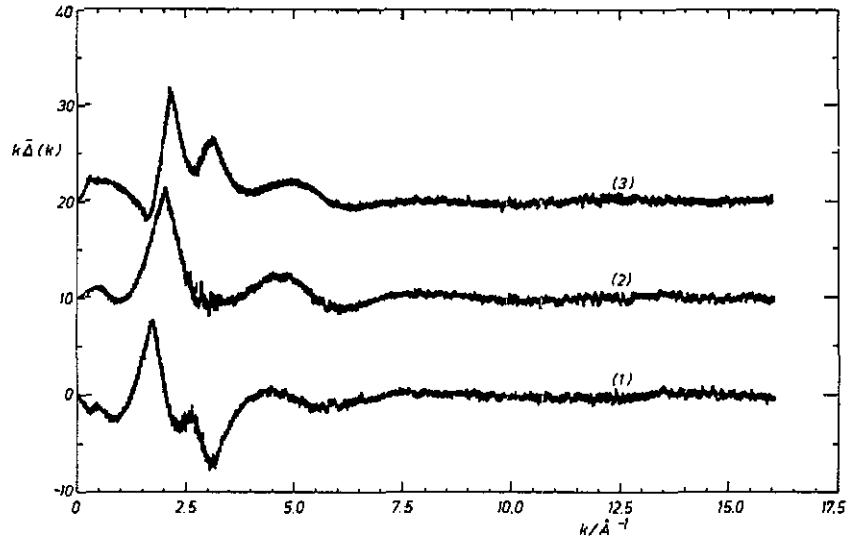

Figure 4. The first-order difference functions, $k\tilde{\Delta}(k)$, for 1M $NaBrO_3/ClO_3$. Curve 1, results for solution (VI – IV); curve 2, those for solutions (I – IV) (displaced by 10 e^2 $Å^{-1}$); curve 3, those for solutions (I – VI) (displaced by 20 e^2 $Å^{-1}$).

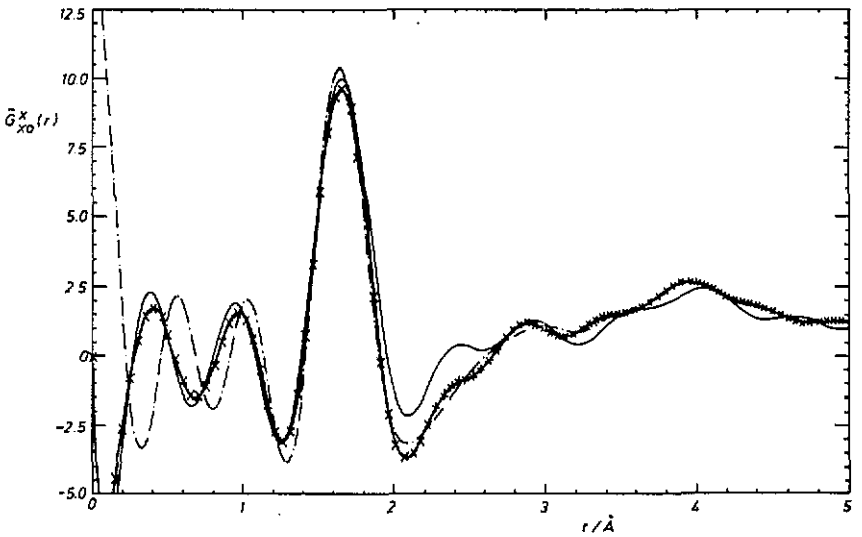

Figure 5. The x-ray first-order difference distribution function, $\tilde{G}^{x}_{XO}(r)$, for 1M $NaNO_3/BrO_3$ solutions. ——, solutions (I – III); x — x, solutions (III – II); — · —, solutions (I – II).

identified by Neilson and Enderby (1982).

Figure 3 shows $k\tilde{\Delta}(k)$ for IV – II, IV – V, and V – II. There is an obvious disagreement with $k\tilde{\Delta}(k)_{IV-V}$ which is out of phase with the other two differences. Thus there is an obvious difference in the structure of the three solutions, and isomorphic behaviour is not observed. Similarly, figure 4 shows $k\tilde{\Delta}(k)$ for I – IV, I – VI and VI – IV. Again, one of the differences, $k\tilde{\Delta}(k)_{I-IV}$ is out of phase with the other two

Table 4. X–O parameters for each $\tilde{G}^{x}_{XO}(r)$ for the 1M $NaNO_3/BrO_3$ solutions. r_1, r_2 and r_3 are due to X–water interactions.

	Intramolecular		Intermolecular		
	r_{XO} (Å)	n_{XO}	r_1 (Å)	r_2 (Å)	r_3 (Å)
$\tilde{G}^{x}_{I-II}(r)$	1.63(1)	3.09(1)		2.98(1)	3.95(1)
$\tilde{G}^{x}_{III-II}(r)$	1.63(1)	2.69(1)	2.55(1)	2.88(5)	3.94(1)
$\tilde{G}^{x}_{I-III}(r)$	1.63(1)	3.74(1)	2.39(1)	3.09(1)	3.86(1)

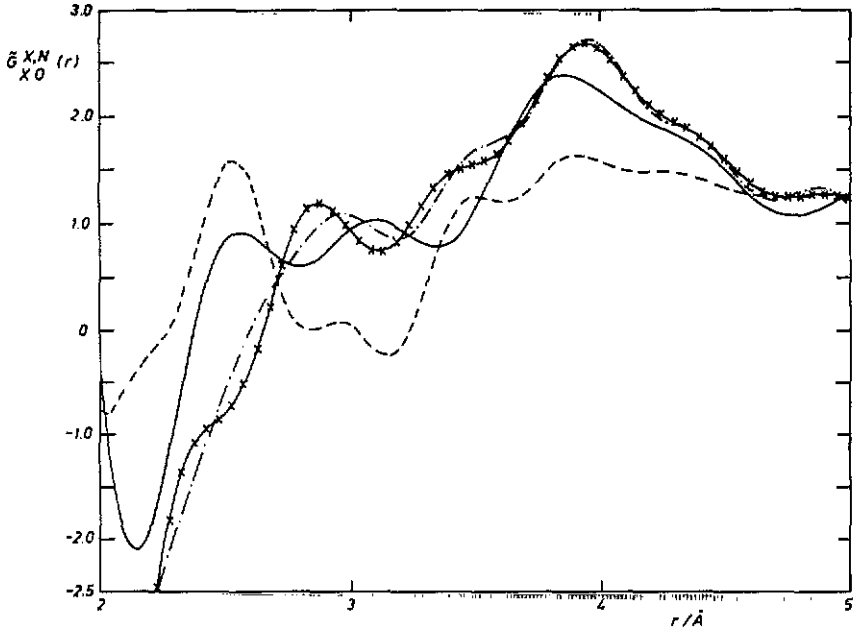

Figure 6. The three x-ray first-order difference distribution functions for 1M $NaNO_3/BrO_3$ compared with the nearest $G^{n}_{XO}(r)$ obtained from 4m $Ni(NO_3)_2$, as measured by Howell (1990) using the first-order difference method of neutron diffraction (– – –). $\tilde{G}^{x}_{XO}(r)_{I-II}$ is denoted by — · —, $\tilde{G}^{x}_{XO}(r)_{I-III}$ by ——, and $\tilde{G}^{x}_{XO}(r)_{III-II}$ is denoted by x.

differences and thus it can be concluded that isomorphic behaviour is not observed.

These results show that only the NO_3^- and BrO_3^- ions are isomorphic since the first-order differences, $\tilde{G}^{x}_{XO}(r)$, are very similar. The self-consistency of the three $\tilde{G}^{x}_{XO}(r)$ is then checked, and when they are compared, figure 5, they are found to agree very well. The maximum values of k in k-space are 13.0, 12.0 and 11.0 $Å^{-1}$ for $\tilde{G}^{x}_{XO}(r)_{I-II}$, $\tilde{G}^{x}_{XO}(r)_{III-II}$ and $\tilde{G}^{x}_{XO}(r)_{I-III}$ respectively. The results given in table 4 for r^{x}_{XO} (intramolecular) and n^{x}_{XO} show agreement within error. The average values are 1.63(1) Å and 3.17(54) respectively. The peaks between 2 and 5 Å are also in agreement, and the average values are, 2.90(8) Å and 3.90(6) Å, see table 4. To further confirm isomorphic behaviour, the x-ray result is compared with the neutron distribution function $G^{n}_{XO}(r)$ of Howell (1990), figure 6, and, allowing for the fact that the weighting for the hydration peaks are different for x-ray diffraction and neutron

scattering, the intermolecular structure appears similar. The data is shown between 2 Å and 5 Å , and the corresponding peaks are at 2.90(8) Å (x-ray) and 3.09 Å (neutron), 3.90(6) Å (x-ray) and 3.96 Å (neutron), with shoulders at 3.45(5) Å (x-ray) and 3.51 Å (neutron), 4.36(6) Å (x-ray) and 4.3 Å (neutron). There is also a peak at an average value of 2.48(8) Å (x-ray) which is not seen in the $\tilde{G}^{x}_{XO}(r)_{I-II}$ shown in figures 5 and 6. When the maximum value of k is reduced to 10 $Å^{-1}$, this peak appears at 2.66(1) Å, but the resolution of the main peaks is worse. Hence the data shown in these figures is taken with respect to the best resolution obtainable. The position of this peak agrees within error with the neutron result at 2.53 Å. These peaks are attributed to ion–water interactions.

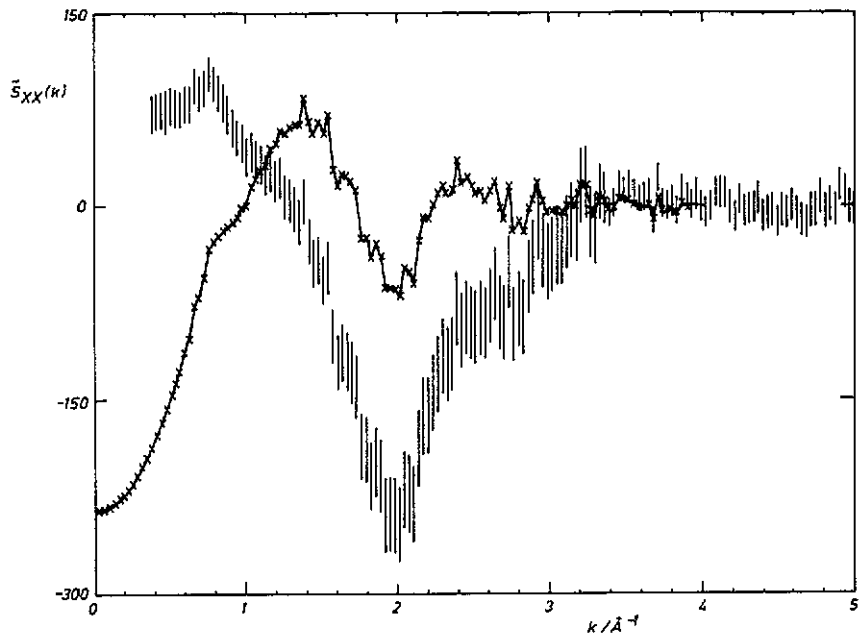

Figure 7. The function $\tilde{S}_{XX}(k)$ in 1M $NaNO_3/BrO_3$ measured by the second-order difference method of x-ray diffraction. The raw data are shown as points with error bars, and the back transform of $\tilde{g}_{XX}(r)$ having been cut off below 4.8 Å is denoted by x — x.

4.2. Calculation of $\tilde{S}_{XX}(k)$ and $\tilde{g}_{XX}(r)$

Having established isomorphism between NO_3^- and BrO_3^-, a second-order difference, $\tilde{S}_{XX}(k)$, was made. This was done by using equation (21) for each pair of first-order differences, i.e., $\tilde{S}_I(k) - \tilde{S}_{II}(k)$, $\tilde{S}_I(k) - \tilde{S}_{III}(k)$ and $\tilde{S}_{III}(k) - \tilde{S}_{II}(k)$. Here the difference between $\tilde{S}_I(k) - \tilde{S}_{II}(k)$ and $\tilde{S}_I(k) - \tilde{S}_{III}(k)$ is presented. Using the extrapolation to $\tilde{S}$(k=0)

$$\tilde{S}_{XX}(k_{j+1}) = \tilde{S}_{XX}(k=0) + 0.2(\tilde{S}_{XX}(k_j) - \tilde{S}_{XX}(k=0)). \tag{22}$$

$\tilde{S}_{XX}(0)$ was calculated to be −234.0 from the last usable datum point at k = 0.5023 $Å^{-1}$. $\tilde{S}_{XX}(k)$ is shown by the bars in figure 7. Residuals of the X–O and

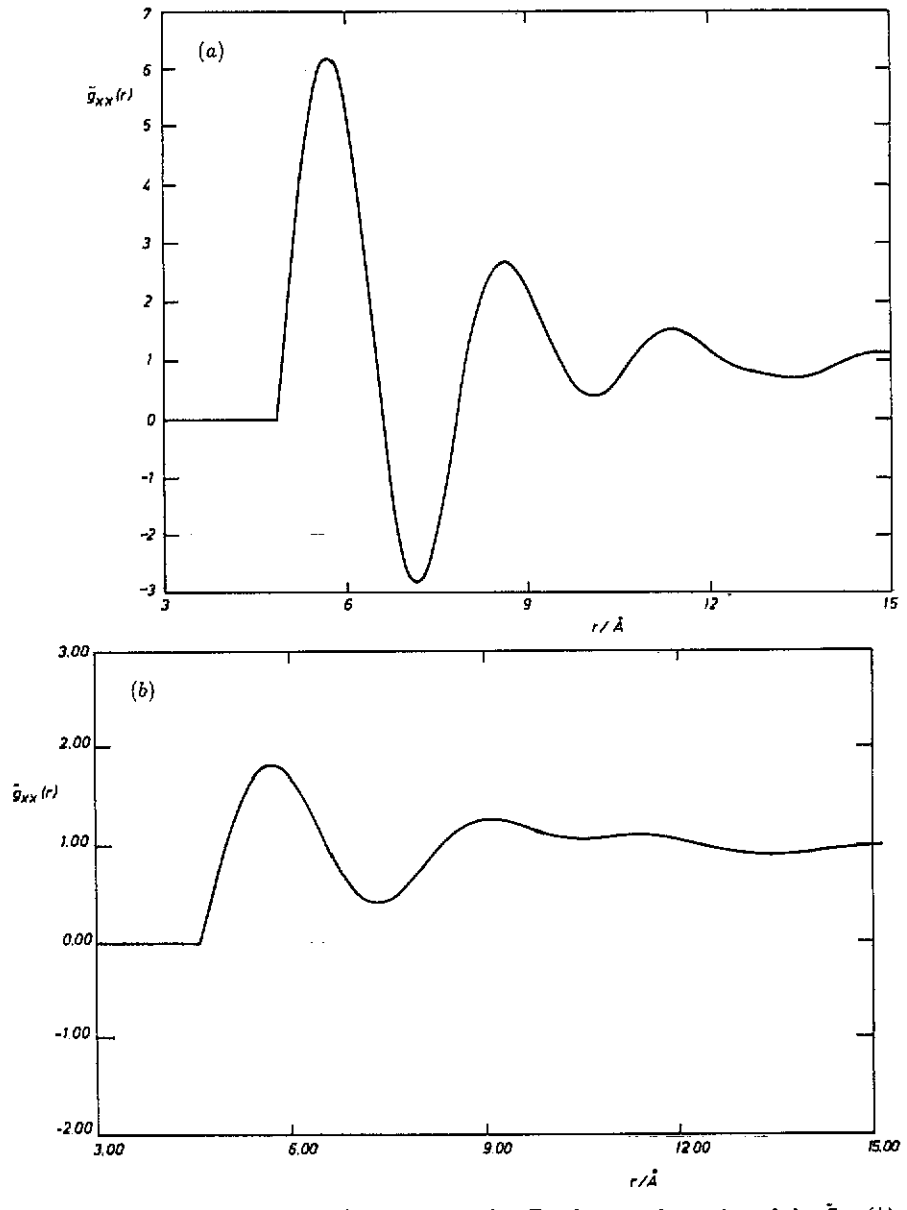

Figure 8. This is the resultant $\tilde{g}_{XX}(r)$ after Fourier transformation of the $\tilde{S}_{XX}(k)$, × — × shown in figure 7, multiplied by (*a*) $e^{-0.05k^2}$ and (*b*) $e^{-0.5k^2}$.

O–H correlations were present in the $\tilde{g}_{XX}(r)$ obtained from the raw data. This could be due to an error of $\approx 2\%$ in the normalization of the difference functions, or a slight departure from isomorphism. These features are removed by setting $\tilde{g}_{XX}(r)$ to zero below 4.8 Å (where the curve cuts the ordinate axis) and backtransforming to give the second $\tilde{S}_{XX}(k)$ shown as × and —— in figure 7. The resultant $\tilde{g}_{XX}(r)$ is the Fourier transform of × — × of figure 7, which has been multiplied by $\exp(-0.05k^2)$ and is shown in figure 8(*a*). The negative peak at 7 Å is removed by smoothing × — × of figure 7 by $\exp(-0.5k^2)$, figure 8(*b*). The main peak is at 5.7 Å and is followed by

two smaller peaks at 8.3 Å and 10.9 Å . The distance of closest approach is taken to be the point at which the data crosses the ordinate axis, and is ≈ 4.8 Å. Similar large peaks at $\approx 5/6$ Å have been obtained in $\tilde{g}_{NiNi}(r)$ for both 1M $Ni/Mg(NO_3)_2$ and 1M $Ni/Mg(SO_4)$, (Burke 1989), which we think can either be due to inexact isomorphic behaviour resulting in inexact cancellation of the water–water terms, or due to an ion–ion interaction occuring much closer than has been previously realised (Skipper 1987, Skipper *et al* 1989). Certainly the negative peak in figure 8(*a*) casts doubt on the $\tilde{g}_{XX}(r)$ presented. The methods of analysis and experimentation (section 3) will inevitably cause systematic errors large enough to introduce problems at the second-order difference stage, where we are working close to the statistical errors of the data, thus producing unphysical peaks and troughs. This will be discussed further in more detail in a future paper on isomorphic behaviour of Ni^{2+} and Mg^{2+} with complex counter-ions.

However, the peak positions are reasonable since the theoretical limit of closest approach is 3.8 Å (i.e., two hard spheres touching each other), and theoretically, if the ions lie at the corners of a BCC unit cell without any forces between them, they would be ≈ 12 Å apart.

5. Conclusions

In conclusion, the above experiments show that x-ray diffraction with isomorphic substitution can be extended to aqueous solutions containing complex ions. It is found that only the NO_3^- and BrO_3^- ions are isomorphic and a second-order difference is determined. The ion–ion distances lie within the theoretical limits of closest approach and the furthest possible distance at the corner of a BCC unit cell.

However, the NO_3^- and ClO_3^- and ClO_3^- and BrO_3^- pairs are not isomorphic even though the former pair are analogues in botanical terms and the latter pair are more similar in structure and have a closer ion–O distance. Thus on the basis of the results presented above it is likely that the effective chemical radii of the ions is more important in determining isomorphic pairs.

Acknowledgments

We wish to thank SERC for its continuing support of our research, Mr Ian Howell for his neutron data (4.3m $NiNO_3$) and Mr P M Gullidge for preparation of the samples for the neutron experiment. We also benefitted from discussions with Professor J E Enderby and Miss P A M Walker. One of us (AKA) wishes to thank the University of Delhi for the grant of study leave.

References

Adya A K and Neilson G W 1991 A structural study of $Rb^+(aq)$ and $Tl^+(aq)$ by the isomorphic substitution technique of x-ray diffraction *J. Phys.: Condens. Matter* (manuscript in preparation)

Bol W, Gerrits G J A and van Panthaleon van Eck C L 1970 The hydration of divalent cations in aqueous solution. An x-ray investigation with isomorphic substitution *J. Appl. Phys.* **3** 486

Burke C A E 1989 Ion–ion and ion–water correlations for some aqueous solutions *PhD Thesis* University of Bristol

Burke-Laing M and Trueblood K N 1977 Sodium chlorate: precise dimensions for the ClO_3^- ion *Acta Crystallogr.* B **33** 2698–9

Caminiti R, Licheri G, Piccaluga G, and Pinna G 1980 Interactions and structure in aqueous $NaNO_3$ solutions *J. Chem. Phys.* **72** 4522

Cromer D T 1969 Compton scattering factors for aspherical free atoms *J. Chem. Phys.* **50** 4857

Cullity B D 1956 *Elements of X-ray Diffraction* (Reading, MA: Addison-Wesley)

Deane-Drummond C E and Glass A D M 1982 Nitrate uptake into barley (hordeum vulgare) plants. A new approach using $^{36}ClO_3^-$ as an analogue for NO_3^- *Plant Physiol.* **70** 50–4

Enderby J E and Neilson G W 1981 *Rep. Prog. Phys.* **44** 593–653

Habenschuss A and Spedding F H 1979 The coordination (hydration) of rare earths in aqueous chloride solutions from X-ray diffraction *J. Chem. Phys.* **70** 2797

Handbook of Chemistry and Physics 1988 69th edn, ed R C Weast, M J Astle and W H Beyer (Boca Raton, FL: Chemical Rubber) p B-129

Howe R A, Howells W S and Enderby J E 1974 Ion distribution and long-range order in concentrated electrolyte solutions *J. Phys. C: Solid State Phys.* **7** L111

Howell I 1990 private communication

Huheey J E 1978 *Inorganic Chemistry* 2nd edn (New York: Harper and Row) p 74

International Tables for X-ray Crystallography 1962 vol 3, ed C H MacGillavry and G D Rieck (Birmingham: Kynoch) p 250

Johansson G and Caminiti R 1986 The hydration of tungstate and molybdate ions in aqueous solutions *Z. Naturf.* **41** 1325–9

Neilson G W and Enderby J E 1979 Neutron and x-ray diffraction studies of concentrated aqueous electrolyte solutions *R. Soc. Chem. Ann. Rep.* C p 185

—— 1982 The structure around nitrate ions in concentrated aqueous solutions *J. Phys. C: Solid State Phys.* **15** 2347

Sandström M, Neilson G W, Johansson G and Yamaguchi T 1985 Ag^+ hydration in perchlorate solutions *J. Phys. C: Solid State Phys.* **18** L1115

Skipper N T 1987 The alkali metal ions in aqueous solutions *PhD Thesis* University of Bristol

Skipper N T, Cummings S C, Neilson G W and Enderby J E 1986 Ionic structure in aqueous electrolyte solution by the difference method of x-ray diffraction *Nature* **321** 52–3

Skipper N T and Neilson G W 1989 X-rays and neutron diffraction studies on concentrated aqueous solutions of sodium nitrate and silver nitrate *J. Phys.: Condens. Matter* **1** 4141–54

Skipper N T, Neilson G W and Cummings S C 1989 An x-ray diffraction study of Ni^{2+}(aq) in electrolyte solution by isomorphic substitution *J. Phys.: Condens. Matter* **1** 1

Soper A K, Neilson G W, Enderby J E and Howe R A 1977 A neutron diffraction study of hydration effects in aqueous solutions *J. Phys. C: Solid State Phys.* **10** 1793

Templeton D H and Templeton L K 1985 Tensor x-ray optical properties of the bromate ion *Acta Crystallogr.* A **41** 133–42

Waddington T C 1959 *Adv. Inorg. Chem. Radiochem.* **1** 180

Walker P A M, Lawrence D G, Neilson G W and Cooper J 1989 The structure of concentrated aqueous ammonium nitrate solutions *J. Chem. Soc. Faraday Trans.* I **85** 1365–72

Wyckoff R W G 1964 *Crystal Structures* vol 2, 2nd edn (New York: Wiley) ch VII, pp 2–6

Yatsimirskii K B 1947 *Izv. Akad. Nauk SSSR, Otdel, Khim. Nauk.* 453

—— 1948 *Izv. Akad. Nauk SSSR, Otdel, Khim. Nauk.* 398